Calcium isotope sources and fractionation during melt–rock interaction in the lithospheric mantle: Evidence from pyroxenites, wehrlites, and eclogites

Article *in* Chemical Geology · June 2019

DOI: 10.1016/j.chemgeo.2019.06.010

CITATIONS
3

READS
115

7 authors, including:

Dmitri Ionov
Université de Montpellier
157 PUBLICATIONS **6,798** CITATIONS
SEE PROFILE

Hongli Zhu
Institute of Oceanography
15 PUBLICATIONS **142** CITATIONS
SEE PROFILE

Fang Liu
Chinese Academy of Sciences
18 PUBLICATIONS **173** CITATIONS
SEE PROFILE

Zhaofeng Zhang
Chinese Academy of Sciences
79 PUBLICATIONS **1,003** CITATIONS
SEE PROFILE

Chemical Geology 524 (2019) 272–282

Contents lists available at ScienceDirect

Chemical Geology

journal homepage: www.elsevier.com/locate/chemgeo

Calcium isotope sources and fractionation during melt-rock interaction in the lithospheric mantle: Evidence from pyroxenites, wehrlites, and eclogites

Jin-Ting Kang (康晋霆)[a,b], Dmitri A. Ionov[a,c], Hong-Li Zhu[a,d], Fang Liu[a], Zhao-Feng Zhang[a,*], Zhe Liu[a], Fang Huang[b,*]

[a] State Key Laboratory of Isotope Geochemistry, Guangzhou Institute of Geochemistry, Chinese Academy of Sciences, Guangzhou 510640, China
[b] CAS Key Laboratory of Crust-Mantle Materials and Environments, School of Earth and Space Sciences, University of Science and Technology of China, Hefei 230026, China
[c] Géosciences Montpellier, Université de Montpellier, Montpellier 34095, France
[d] Center of Deep Sea Research, Institute of Oceanology, Chinese Academy of Sciences, Qingdao 266071, China

ARTICLE INFO

Editor: Catherine Chauvel

Keywords:
Ca isotopes
Mantle metasomatism
Wehrlite
Eclogite
Pyroxenite

ABSTRACT

To investigate the effects of melt metasomatism on Ca isotope fractionation in the upper mantle, we report data for xenoliths of mantle rocks including composite peridotites (lherzolites and coexisting pyroxenite veins), wehrlites as well as eclogites and their minerals. The $\delta^{44/40}$Ca in clinopyroxenes (cpx) are ~0.3‰ lower than in coexisting garnets in eclogites from the Udachnaya kimberlite in the central Siberian craton, likely due to equilibrium isotope fractionation controlled by mineral structure. The $\delta^{44/40}$Ca in the pyroxenite veins (cumulates from mafic melts) and their host peridotites from Tariat in Mongolia range from 0.88‰ to 1.05‰ and are close to the Bulk Silicate Earth (BSE) value (0.95 ± 0.05‰). Calcium-Fe-rich low-orthopyroxene lherzolites and wehrlites (LW series) from Tok in the SE Siberian craton were formed by reaction of lherzolites and harzburgites with percolating silica-undersaturated melts. The $\delta^{44/40}$Ca (0.65‰–0.87‰) in the Tok peridotites are negatively correlated with Ca/Al, $(Gd/Yb)_N$ and positively with Mg# (indices of melt-rock reaction degrees). The $\delta^{44/40}$Ca ratios in the LW series rocks are lighter than the BSE estimate, and similar to $\delta^{44/40}$Ca in their host basalt and an olivine-cpx cumulate (0.70‰–0.76‰). These observations on the Tok suite can be explained by reaction of refractory peridotite protoliths with melts derived from mixed eclogite and peridotite sources. Overall, the $\delta^{44/40}$Ca variations in eclogites, wehrlites, and various rocks related to silicate melts in the mantle, demonstrate that melt metasomatism plays an important role in producing mantle Ca isotope heterogeneity. The data for coexisting garnet and cpx in eclogites outline a potential for garnet to affect Ca isotope inter-mineral and solid-melt fractionation in the mantle.

1. Introduction

Mantle metasomatism combines a range of processes taking place when migrating melts or fluids react with host fertile or refractory peridotites, which could change the chemical and isotope compositions of mantle rocks and minerals (e.g., Bailey, 1982; Bodinier and Godard, 2003). Disentangling the complex records of metasomatism involving a range of sources and media is crucial to tracing mantle evolution. Radiogenic isotopes may be used to date mantle events, but tracing their ratios in the initial materials and products of metasomatic events is problematic because they evolve with time as a function of ratios of parent-daughter elements.

Calcium is a major element in the most common mantle rocks (peridotite, pyroxenite, and eclogite) and is mobile in metasomatic agents like silicate and carbonate melts/fluids (e.g., Ionov et al., 1993; Ionov et al., 1996; Rudnick et al., 1993; Yaxley et al., 1991). Rapid improvements of analytical techniques in the last two decades made it possible to analyze non-traditional stable isotopes in geological materials, and considerable Ca isotopic variations in mantle rocks have been found recently (Huang et al., 2010; Kang et al., 2016, 2017; Zhao et al., 2017; Chen et al., 2018, 2019; Ionov et al., 2019). Some of these variations have been attributed to metasomatism (e.g., Ionov et al., 2019 and references therein), but the range and mechanisms for Ca isotope variations in metasomatic processes continue to be debated. Better knowledge of these topics is essential to applying the Ca isotope system to mantle geochemistry, which may provide important additional constraints on mantle metasomatism and its role in shaping the global reservoirs of the Earth.

* Corresponding authors.
E-mail addresses: zfzhang@gig.ac.cn (Z.-F. Zhang), fhuang@ustc.edu.cn (F. Huang).

https://doi.org/10.1016/j.chemgeo.2019.06.010
Received 22 January 2019; Received in revised form 16 May 2019; Accepted 10 June 2019
Available online 14 June 2019

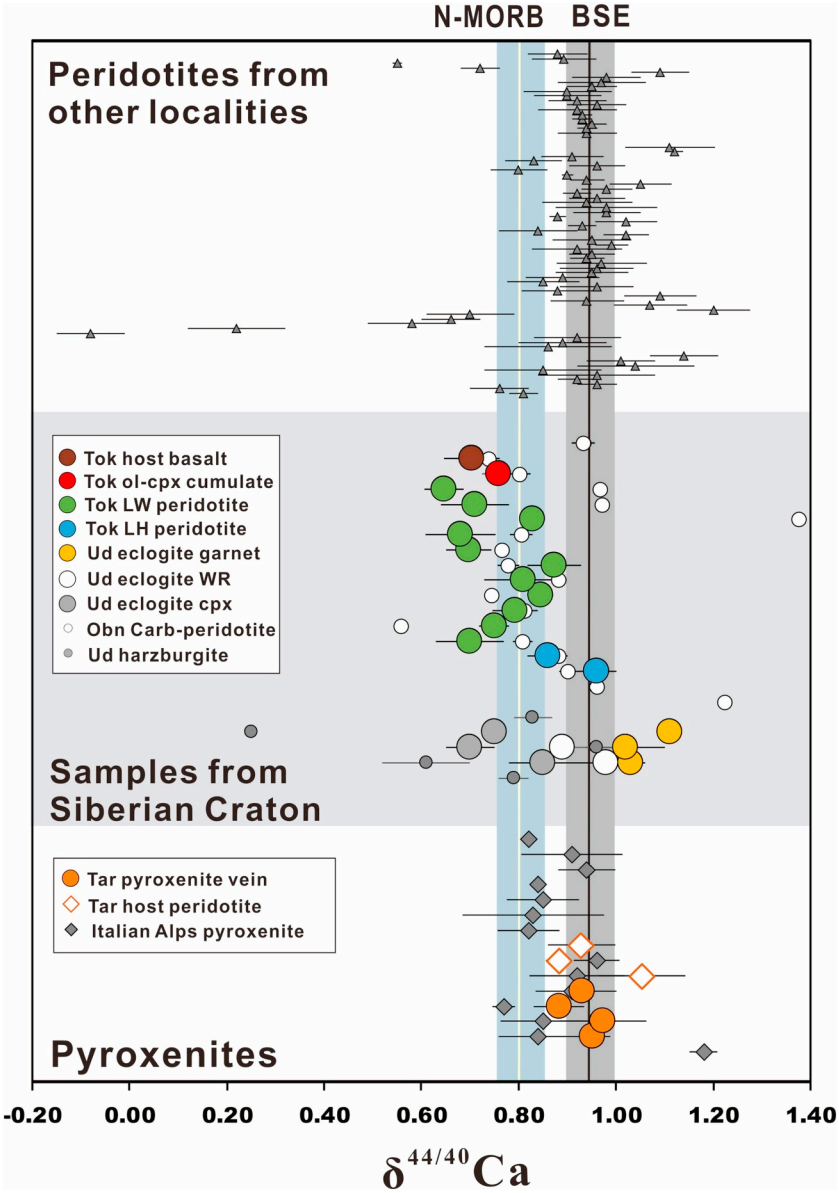

Fig. 1. Calcium isotope composition ($\delta^{44/40}$Ca) for samples in this study (large symbols, data from Table 1): whole-rock (WR) peridotite xenoliths from Tok (LH, lherzolite-harzburgite series; LW, lherzolite-wehrlite series, olivine-cpx cumulate and host basalt) as well as WR and mineral (garnet and cpx) data for three eclogite xenoliths from Udachnaya, and pyroxenite veins and their host lherzolites from Tariat. Error bars are 2SE. Also shown (vertical lines) are the BSE value (0.94 ± 0.05‰) after Kang et al. (2017), the $\delta^{44/40}$Ca range (0.75–0.86‰) for N-MORB after Zhu et al. (2018b). Siberian craton samples are from Ionov et al. (2019) for Obnazhennaya carbonatite peridotites and Kang et al. (2017) for Udachnaya harzburgites. Alps pyroxenites are from Chen et al. (2019). Peridotites from other localities include China xenoliths from Kang et al. (2016), Zhao et al. (2017) and Chen et al. (2018), Italian massif from Chen et al. (2019), Mongolia xenoliths from Kang et al. (2017) and USGS peridotite standard from Amini et al. (2009). For locality abbreviations refer to the caption of Fig. 2 and for color codes refer to the online version of the paper.

To date, near 1.5‰ fractionation of $\delta^{44/40}$Ca has been documented in metasomatized peridotites and their minerals (Fig. 1, Chen et al., 2018; Huang et al., 2010; Ionov et al., 2019; Kang et al., 2017; Kang et al., 2016; Zhao et al., 2017). These isotopic variations have been interpreted to result from: (1) equilibrium inter-mineral fractionation controlled by mineral structures and temperature (e.g., Huang et al., 2011; Kang et al., 2017; Liu et al., 2017a); (2) metasomatism by carbonatite or carbonate-rich melts/fluids (e.g., Feng et al., 2014; Macris et al., 2015; Wang et al., 2017b; Young et al., 2009); and (3) kinetic isotope fractionation driven by chemical diffusion (e.g., Richter et al., 2009; Zhao et al., 2017). However, because the Ca isotope data for mantle rocks remain rare, and because nearly all the samples studied are lherzolites and harzburgites, the scale of mantle Ca isotope heterogeneity and the fractionation mechanisms during mantle metasomatism are not sufficiently constrained as yet. Among the important unresolved questions are the effects of silicate melts (the most common metasomatic media in mantle, e.g., Bodinier et al., 1990), on Ca isotopes, in particular for rocks (pyroxenites, wehrlites), containing the highest melt contributions.

To better constrain and understand Ca isotope variations related to mantle metasomatism, in particular interaction of silicate melts with lithospheric peridotites, we report Ca isotopic compositions in two suites of mantle xenoliths. Peridotites from Tok in the southeastern Siberian craton represent different degrees of reaction of initial residual mantle with percolating silicate melts, whereas peridotites from Tariat in Mongolia contain pyroxenite veins formed by crystallization of silicate melts in mantle conduits. We also studied three eclogite xenoliths from the Siberian craton (Udachnaya), and garnet and clinopyroxene (cpx) separated from these eclogites. This work presents the first Ca isotope data for eclogite xenoliths, an important component of cratonic mantle believed to originate from recycled ancient crust, and for wehrlites, products of extensive melt metasomatism. Our data on the eclogites show that clinopyroxene is 0.3‰ lighter than coexisting garnet due to equilibrium inter-mineral fractionation. We calculate that partial melts from eclogite sources may be ~0.3‰ lighter than melts from fertile peridotite sources, and that eclogite-derived melts may produce low $\delta^{44/40}$Ca in metasomatized mantle.

2. Geological background and sample description

2.1. Xenolith localities and their tectonic settings

Twenty-two mantle xenoliths in this study are from three localities in the central and northeastern Asia (Fig. 2). Three eclogite xenoliths are from the Udachnaya kimberlite in the central Siberian craton. The ~220 km thick lithosphere (Ionov et al., 2010) in the region formed in two stages, at ~2.8 Ga and ~2.0 Ga, based on Re-Os model ages of refractory mantle peridotites (Ionov et al., 2015), Pb-Pb ages of eclogites (Jacob et al., 1994) and U-Pb dating of zircons from ancient crustal rocks (Moyen et al., 2017).

The largest number of samples (15) is from the late Cenozoic Tok volcanic field in the Stanovoy block of the Aldan shield at the SE margin of the Siberian craton (Ionov et al., 2005b). The lithosphere in the area probably formed at the same time as in the center of the craton, but it experienced repeated tectonic reactivation since the Mesozoic and has been thinned to < 100 km, possibly in relation to subduction in the NW Pacific (Ionov et al., 2006a). The peridotite xenoliths were found in alkali basaltic lava flows. They differ from kimberlite-hosted refractory peridotites from the central craton (Ionov et al., 2010) by lower Mg# [$Mg/(Mg + Fe)_{at}$] (≤0.92 vs. 0.92–93), and the absence of garnet-bearing and deformed (sheared) rocks.

Four composite peridotite xenoliths are from the late Cenozoic Tariat volcanic field in the northern Hangay Mountains in central Mongolia, part of the mainly Paleozoic Central Asian Orogenic Belt. They are hosted by alkali basaltic breccia at the Shavaryn-Tsaram eruption center (Ionov et al., 1998).

2.2. Xenolith rock types and chemical compositions

The Udachnaya eclogite xenoliths were selected to cover a range of modal and major oxide compositions for eclogites from this locality (Agashev et al., 2018; Jacob et al., 1994). They are coarse-grained bimineral rocks with roughly equal proportions of well-preserved garnet and cpx (omphacite). The major oxide variations in the two minerals are very broad, with Mg# of 0.42–0.77, 4.7–12.8 wt% CaO and 0.04–1.57 wt% Cr_2O_3 for garnet, and 14.2–20.6 wt% CaO, 1.7–9.1 wt% Al_2O_3 and 1.6–6.2 wt% Na_2O for the cpx (Table S1).

The fifteen samples from Tok include 13 mantle peridotites, a host basaltic lava (Mg# 0.63) and an olivine-clinopyroxene cumulate xenolith (Mg# 0.83) formed from the host basaltic magma. Their major element compositions were reported in Ionov et al. (2005a) and Ionov et al. (2005b), trace element data in Ionov et al. (2006a) and Os-Sr-Hf-Nd isotope data in Ionov et al. (2006b). The mantle peridotites from Tok are divided in two series based on modal and chemical compositions (Ionov et al., 2005a; Ionov et al., 2005b). Two samples in this study belong to the lherzolite–harzburgite (LH) series, which groups residues of low to high degrees of melt extraction from fertile mantle (Mg# 0.89–0.92). Eleven xenoliths belong to the lherzolite–wehrlite (LW) series characterized by low Mg# (0.84–0.89), high modal olivine (66–84%) and high modal ratios of cpx to orthopyroxene (opx). The LW series rocks were produced by reaction of partial melting residues (LH series) with evolved, low-Mg#, Ca-rich under-saturated silicate melts, which caused replacement of opx by cpx and Fe-enrichments (Ionov et al., 2005a). The LH and LW series rocks also contain fine-grained interstitial materials including phosphates, alkali feldspar and Na-rich cpx formed from late-stage, water-poor fluids (Ionov et al., 2006a). The photomicrographs of LW samples and olivine-cpx cumulate can be found in Ionov et al. (2005a) and Ionov et al. (2005b). Essential petro-geochemical data on the Tok xenoliths in this study are provided in Table S2.

Three out of the four xenoliths from Tariat are composite, i.e. they consist of two rock types with distinct origins. Each xenolith is made up of coarse spinel lherzolite crosscut by a coarse-grained pyroxenite vein 2–3 cm thick with abrupt, non-gradational contacts. The veins in two

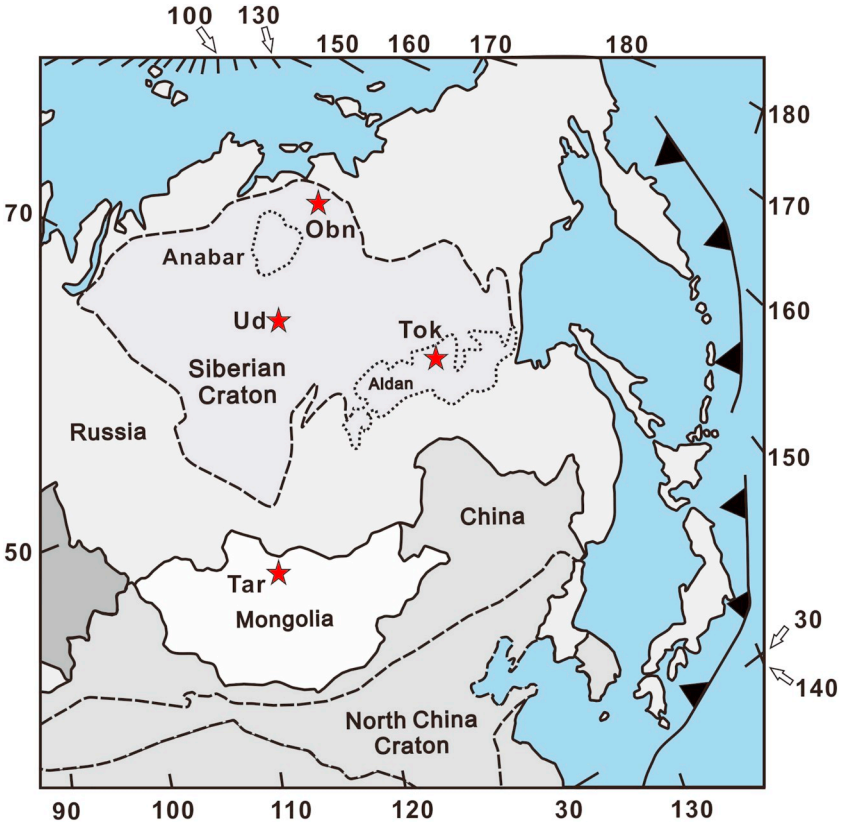

Fig.2. A sketch map of the central and northeastern Asia. Abbreviations: Tok, Tokinsky Stanovik Range; Ud, Udachnaya; Tar, Tariat; Obn, Obnazhennaya.

Table 1
Ca isotope compositions in samples from this study and international reference samples.

Sample	Rock type	Locality	GPS location	$\delta^{44/40}$Ca					Mean	2SD	2SE	n	Data source[c]
				1[a]	2	3	4	R[b]					
LH series xenoliths from Tok													
9506-0	Spl Hz	Tok	55°38′N; 130°06′	0.90	1.03	0.99	0.94	0.95	0.96	0.10	0.04	5	(1)
9506-1	Spl Lh	Tok		0.89	0.87	0.82			0.86	0.07	0.04	3	(1)
LW series xenoliths from Tok													
9502-1	Low opx spl Lh	Tok	55°38′N; 130°06′	0.64	0.76	0.7			0.70	0.12	0.07	3	(2)
9502-3	Spl Wh	Tok		0.77	0.76	0.72			0.75	0.05	0.03	3	(2)
9502-4	Spl Wh	Tok		0.75	0.83	0.80			0.79	0.08	0.05	3	(2)
9502-10	Low opx Spl Lh	Tok		0.84	0.83	0.87			0.85	0.04	0.02	3	(2)
9503-2	Low opx Spl Lh	Tok		0.89	0.78	0.76			0.81	0.14	0.08	3	(2)
9503-22	Spl Wh	Tok		0.89	0.82	0.91			0.87	0.09	0.05	3	(2)
9507-6	Spl Wh	Tok		0.74	0.69	0.66			0.70	0.08	0.05	3	(2)
9508-10	Spl Wh	Tok		0.66	0.63	0.75			0.68	0.12	0.07	3	(2)
9510-1	Spl Wh	Tok	55°37′N; 130°06′	0.85	0.85	0.80		0.82	0.83	0.05	0.02	4	(2)
9510-3	Spl Wh	Tok		0.78	0.67	0.68			0.71	0.12	0.07	3	(2)
9510-11	Spl Lh	Tok		0.61	0.65	0.68			0.65	0.07	0.04	3	(2)
Ol-Cpx cumulate xenolith and basalt hosting Tok xenoliths													
9508-14	Ol-Cpx cumulate	Tok	55°38′N; 130°06′	0.73	0.79	0.76			0.76	0.06	0.03	3	(2)
9508-1b	host basalt	Tok		0.67	0.76	0.68			0.70	0.10	0.06	3	(2)
Mineral separates and WR of eclogites from Udachnaya													
U-400	Cpx	Ud	66°26′N, 112°19′E	0.82	0.82	0.92			0.85	0.12	0.07	3	(4)
	Grt	Ud		1.06	1.00	1.03			1.03	0.06	0.03	3	(4)
	WR	Ud		0.92	1.01	1.02			0.98	0.11	0.06	3	
U-401	Cpx	Ud		0.74	0.65	0.70			0.70	0.09	0.05	3	(4)
	Grt	Ud		0.94	1.05	1.06			1.02	0.13	0.08	3	(4)
	WR	Ud		0.91	0.89	0.88			0.89	0.03	0.02	3	
U-402	Cpx	Ud		0.77	0.73	0.75			0.75	0.04	0.02	3	(4)
	Grt	Ud		1.10	1.11	1.12			1.11	0.02	0.01	3	(4)
Pyroxenite veins and their host lherzolites from Tariat													
S-8	Spl Lh-Px-te	Tar	48°12′N, 100°E	0.90	0.98	0.97		0.96	0.95	0.07	0.04	4	(5)
S-12 lh	Spl Lh	Tar		1.04	0.99	0.89			0.97	0.15	0.09	3	(5)
S-12 vein	Spl Px-te	Tar		1.14	1.03	0.99			1.05	0.16	0.09	3	(5)
4230–15 Lh	Spl Lh	Tar		0.93	0.84			0.88	0.88	0.09	0.05	3	(3)
4230–15 vein	Spl Px-te	Tar		0.91	0.87	0.87			0.88	0.05	0.03	3	(3)
4399-24Lh	Spl Lh	Tar		1.00	0.89	0.90			0.93	0.12	0.07	3	(3)
4399–24 vein	Grt Opx-te	Tar		0.87	0.96	0.95			0.93	0.10	0.06	3	(3)
International reference samples													
AGV-1									0.72	0.06	0.04	3	
BHVO-2									0.80	0.10	0.03	16	
NIST SRM915a									0.02	0.13	0.02	61	
Seawater									1.83	0.11	0.01	68	
NIST SRM915b									0.74	0.09	0.04	6	

Location abbrevations: Tok, Tokinsky Stanovik Range; Tar, Tariat; Ud, Udachnaya.
Rock type abbreviations: Lh, lherzolite; Hz, harzburgite; Wh, wehrlite; Px-te, pyroxenite; WR, whole-rock.
Mineral abbreviations: Grt, garnet; Spl, spinel; Cpx, clinopyroxene; Opx, orthopyroxene; Ol, olivine.
[a] Numbers (1 to 4) represent repeated analyses of the same solution.
[b] R, full-procedure duplicate (repeated dissolution and analysis).
[c] Data sources: (1) Ionov et al. (2005a); (2) Ionov et al. (2005b); (3) Ionov et al. (1998); (4) this work; (5) unpublished data of D. Ionov and R. Carlson.

samples (S-12 and 4230-15) are spinel websterites, the vein in 4399-24 is a garnet orthopyroxenite (Ionov et al., 1998), all of them contain accessory phlogopite. The veins were formed by intrusion and crystallization of mafic silicate liquids in lithospheric peridotites. The Mg# of the veins are close to, or only slightly lower than for the host peridotites indicating that the veins are crystal cumulates from parental liquids equilibrated with fertile to moderately refractory mantle similar to their host peridotites. Sample S-8 has a particular composition transitional between spinel lherzolite and pyroxenite: 39% olivine, 31% opx, 24% cpx, 6% spinel and Mg# 0.89, very similar to that of the host of the vein in xenolith S-12. It may be a hybrid rock, possibly a fertile lherzolite or a melting residue that trapped mafic melt during partial melting.

Overall, the samples from the three localities in this study represent three distinct suites of lithospheric mantle materials, allowing us to examine the behavior of Ca isotopes in silicate melt fractionation and metasomatism, and constrain the Ca isotopic compositions of different mantle lithologies. The Tariat xenoliths are products of mingling of mainly fertile, off-craton lithospheric peridotites with mafic magmas probably akin to DMM-type basalts. The Tok suite enables us to examine the reaction of mantle peridotites with silica-undersaturated, Ca-Fe-rich melts that are out of equilibrium with residual lithospheric mantle. Finally, the Ca isotope composition of eclogite xenoliths are reported here for the first time in order to characterize the minor but important group of rocks existing in the cratonic mantle, and possibly in convecting mantle. Furthermore, the cpx-garnet Ca isotope partitioning in these eclogites may be a key to understand the generation of metasomatic liquids that are out of chemical and isotope equilibrium with normal lithospheric peridotites.

3. Analytical methods

Major element analyses of garnet and cpx in eclogite xenoliths were carried out at the State Key Laboratory of Isotope Geochemistry (SKLIG), Guangzhou Institute of Geochemistry (GIG), Chinese Academy

of Sciences (CAS) with a JEOL JXA-8100 Superprobe. Operating conditions were as follows: 40 kV accelerating voltage, 20 nA beam current, 1 μm beam diameter, counting times of 40 s for peaks and 40 s for background as recommended by Ziberna et al. (2016) and ZAF correction procedure for data reduction. The analytical procedures were described in detail by Huang et al. (2007).

Chemical processing and mass spectrometric analyses of Ca isotopes were also carried out at GIG, CAS. The chemical purification procedure for calcium was described in Zhu et al. (2016, 2018a) and Liu et al. (2017b). Briefly, 10–60 mg of rock powder was weighted. The powder was digested using a 3:1 mixture of concentrated HF and HNO_3 in a 7 ml PFA beaker on a hot plate at 110 °C for 2–3 days. After the digestion, the samples were dried down at 80 °C and refluxed with 6 N HCl several times to remove precipitated CaF_2 until completely dissolved, then evaporated to dryness. The dried residue was finally dissolved in 1.6 N HCl. An aliquot containing ~50 μg Ca was mixed with an appropriate amount of ^{42}Ca-^{43}Ca double spike solution. After adding spikes into sample solutions, they were capped and put on the hotplate overnight to achieve isotopic equilibrium. Spiked sample solution was loaded onto a Teflon column packed with 1 ml pre-cleaned Bio-Rad AG MP-50 (100–200 mesh) resin. Ca was rinsed with 1.6 N HCl media and the column chemistry was carefully calibrated to ensure > 99% Ca yield. The chemical separation procedure was repeated twice to obtain a pure Ca solution. Blanks of the digestion and chemical procedures are < 50 ng, which is insignificant relative to the amount of Ca processed.

Calcium isotopes were analyzed on a thermal ionization mass-spectrometer (Thermo Triton) at the GIG, CAS. Instrumental mass dependent fractionation was corrected using a double-spike method adapted from Heuser et al. (2002). ^{41}K was monitored to correct for isobaric interference of ^{40}K on ^{40}Ca using $^{40}K/^{41}K = 1.7384 \times 10^{-3}$. NIST SRM915a (carbonate standard) and seawater standard (IAPSO) were routinely analyzed during analytical sessions to monitor instrumental stability and reproducibility. The Ca isotope data are expressed relative to NIST SRM915a and reported as $\delta^{44/40}Ca$ (‰) = $[(^{44}Ca/^{40}Ca)_{sample} / (^{44}Ca/^{40}Ca)_{NIST\ SRM\ 915a} - 1]$ in this study.

The internal precision (reproducibility) of $\delta^{44/40}Ca$ values in this study is ± 0.08‰ (2SE) based on 3 repeated measurements of each sample solution. Two standard deviations of average $\delta^{44/40}Ca$ in SRM915a measured in the course of this study is ± 0.13‰ (n = 61), which represents long-term external precision. The values for SRM915a, SRM915b, IAPSO Seawater, and two USGS reference samples (AGV-1 and BHVO-2) analyzed in the same analytical campaign are reported in Table 1. The mean values of $\delta^{44/40}Ca$ obtained for SRM915a and IAPSO Seawater are 0.02 ± 0.13‰ (2SD, n = 61) and 1.83 ± 0.11‰ (2SD, n = 68), respectively; those for AGV-1, BHVO-2 and NIST SRM 915b are 0.72 ± 0.06‰ (2SD, n = 3), 0.80 ± 0.10‰ (2SD, n = 16) and 0.74 ± 0.09‰ (2SD, n = 6), respectively, which are in agreement with data in the literature (e.g., Amini et al., 2009; He et al., 2017; Huang et al., 2010; Magna et al., 2015; Valdes et al., 2014). In addition, full duplicates of 4 samples (9506-0, 9510-1, S-8 and 4230-15Lh) obtained by digestion of duplicate batches of rock powder show good reproducibility within the analytical errors (Table 1). The results of standards and duplicate samples demonstrate the robustness of our analytical methods.

4. Results

Calcium isotope compositions are reported in Table 1 and illustrated in Fig. 1.

The $\delta^{44/40}Ca$ of garnet in the Udachnaya eclogites fall in a narrow range from 1.03 to 1.11‰, and are significantly higher than the $\delta^{44/40}Ca$ values in coexisting cpx (0.70–0.85‰). Whole-rock $\delta^{44/40}Ca$ values measured in two eclogites (U-400 and U-401) are 0.98 ± 0.11‰ (n = 3, 2SD) and 0.89 ± 0.03‰ (n = 3, 2SD) (Fig. 1). Bulk rock estimates calculated for all three eclogites in this study from mineral analyses assuming ~1:1 cpx/garnet ratios (Agashev et al., 2018) range from 0.86‰ to 0.94‰ and are consistent with the measured bulk rock values.

The $\delta^{44/40}Ca$ range in the Tariat pyroxenite veins (0.88–1.05‰) is similar to that for their host peridotites (0.88–0.97‰). In detail, the $\delta^{44/40}Ca$ values for the host lherzolite and the veins are identical in two of the three composite xenoliths, and within uncertainty in the third one. The $\delta^{44/40}Ca$ (0.95 ± 0.07‰, n = 4, 2SD) in xenolith S-8 (intermediate between lherzolite and olivine websterite) falls in the range of the veined peridotites.

The $\delta^{44/40}Ca$ in the thirteen Tok peridotites ranges from 0.65‰ to 0.96‰ (Fig. 1). The $\delta^{44/40}Ca$ values in the two analyzed LH series rocks (0.86‰ and 0.96‰) are at the top of this range (Fig. 1), whereas all but one of the 11 LW peridotites have lower $\delta^{44/40}Ca$ (0.65–0.87‰, with an average of 0.76 ± 0.15‰, n = 11, 2SD) than in the LH rocks (0.86–0.96‰) as well as in all Tariat samples in this study. The olivine-cpx cumulate (0.76 ± 0.06‰, n = 3, 2SD) and host basalt (0.70 ± 0.10‰, n = 3, 2SD) from Tok show relatively light $\delta^{44/40}Ca$ near the bottom of the range for the LW series xenoliths.

5. Discussion

5.1. Calcium isotope composition of Udachnaya eclogites

5.1.1. Calcium isotope fractionation between garnet and clinopyroxene

Our detailed electron microprobe analyses of the Udachnaya eclogites found no significant major element zoning or grain-to-grain variations for garnet and cpx (Table S1) indicating inter-mineral chemical equilibrium, consistent with equilibrated microstructures of the rocks. This suggests that the systematic $\delta^{44/40}Ca$ differences between the garnet and cpx ($\Delta^{44/40}Ca_{grt\text{-}cpx}$ = 0.22–0.34‰) should be attributed to equilibrium inter-mineral isotope fractionation. The existence of significant garnet-cpx Ca isotope fractionation in the eclogites, and possibly in other garnet-bearing mantle rocks, is a major finding of this study and needs to be replicated in eclogites from other worldwide localities.

The existence and magnitude of equilibrium garnet-cpx Ca isotope fractionation in our samples find support in a theoretical study of Huang et al. (2019). The equilibration temperatures (T) for the Udachnaya eclogites estimated from the Fe-Mg exchange method of Ravna (2000) (with pressure assumed to be 5 GPa, Agashev et al., 2018) range from 940 °C to 1247 °C. For this T range, Huang et al. (2019) predict an equilibrium $\Delta^{44/40}Ca_{grt\text{-}cpx}$ of 0.26‰–0.40‰ (Fig. 3). This $\Delta^{44/40}Ca_{grt\text{-}cpx}$ range is very close to the values of 0.17‰–0.36‰ obtained in this study. The uncertainties of these values are estimated to be ± 0.17‰ based on propagated uncertainties of ± 0.13‰ (2SD) for $\delta^{44/40}Ca_{grt}$ and $\delta^{44/40}Ca_{cpx}$. The equilibrium isotope fractionation is generally controlled by chemical bonding environment of Ca in minerals. The Ca−O bond lengths of < 2.40 Å in garnet are lower than in cpx (> 2.43 Å), such that the stronger Ca−O bonding environment in garnets favors heavier isotopes (Beran et al., 1996; Cameron et al., 1973; Sharp et al., 1987; Zhou et al., 2016).

The scale of inter-mineral Ca isotope fractionation may depend on mineral compositions (e.g., Antonelli et al., 2019; Feng et al., 2014; Macris et al., 2015; Schauble, 2011; Wang et al., 2017a; Wang et al., 2017b) in addition to equilibrium temperature and pressure (e.g., Urey, 1947). The recent theoretical work of Feng et al. (2014) and Wang et al. (2017b) revealed that the Ca concentrations in opx may affect the average Ca−O bond length and outlined a negative relationship between CaO in orthopyroxene and $\Delta^{44/40}Ca_{opx\text{-}cpx}$. Furthermore, Schauble (2011) found that elements like Cr, Al, and Co may affect the Mg−O bond length in spinel. This may imply that compositional effects may play an important role in modifying the Ca−O bond length in garnet as well. However, the relatively small range of $\Delta^{44/40}Ca_{grt\text{-}cpx}$ (0.17–0.36‰) in our xenoliths compared to variations by a factor of > 2 in the abundances of several major elements both in the garnet

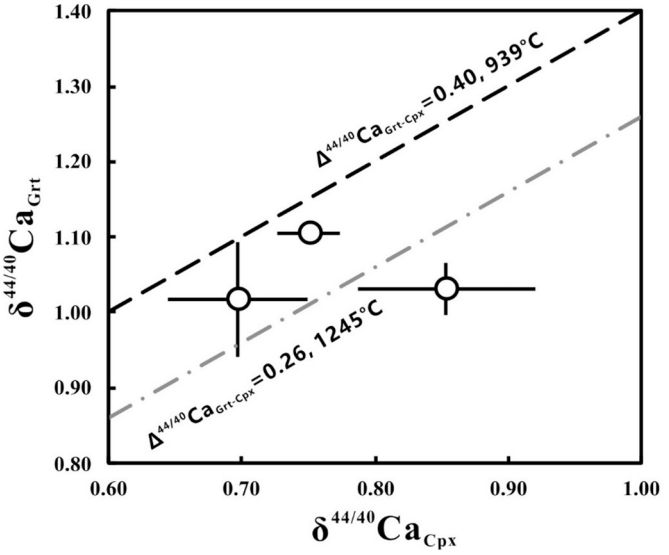

Fig.3. A co-variation plot for $\delta^{44/40}$Ca in coexisting garnet and cpx in Udachnaya eclogites in this study. Error bars are 2SE. The dashed lines are the estimated equilibrium $\Delta^{44/40}Ca_{grt\text{-}cpx}$ at 939 °C and 1245 °C (Huang et al., 2019).

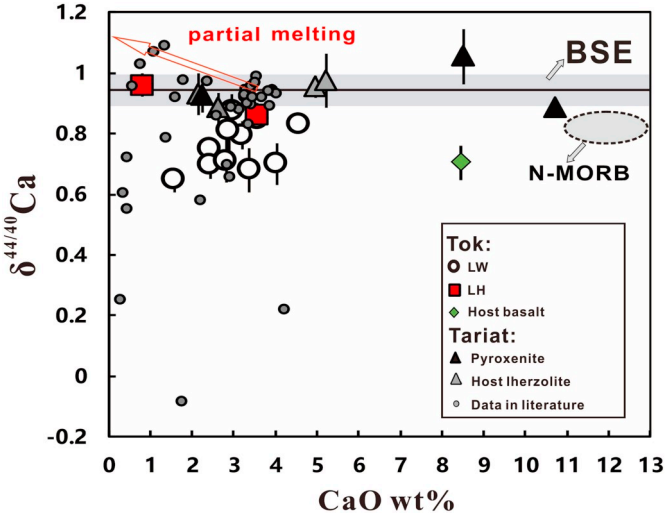

Fig.4. A plot of WR $\delta^{44/40}$Ca vs. CaO for mantle xenoliths from this study in comparison with the BSE range (grey field at 0.94 ± 0.05‰, Kang et al., 2017) and N-MORB (Zhu et al., 2018b). Also shown (small circles) are peridotite data from the literature (Chen et al., 2018; Huang et al., 2010; Kang et al., 2016, 2017; Zhao et al., 2017). Error bars are 2SE. For color codes refer to the online version of the paper.

and in the cpx (Table S1) suggest that compositional effects of major elements on $\Delta^{44/40}Ca_{grt\text{-}cpx}$ may be minor.

Broad $\delta^{44/40}$Ca differences between opx and cpx (up to 1‰), accompanied by large and systematic mineral-scale CaO variations in the pyroxenes, were found in peridotite xenoliths from Yangyuan, eastern China (Zhao et al., 2017). The $\delta^{44/40}$Ca variations were attributed to kinetic diffusion effects in melt-rock reactions, with light isotopes moving faster than heavier isotopes. Such a mechanism implies steep grain-scale chemical gradients (Zhao et al., 2017) and thus is at odds with the absence of major element zoning in mineral grains both in our samples and in previous studies of Udachnaya eclogites (e.g., Snyder et al., 1997) as well as their textural equilibration.

5.1.2. Calcium isotope composition of bulk eclogites

Petrologic and geochemical studies of Udachnaya eclogites reported strong isotope evidence (non-mantle oxygen with $\delta^{18}O_{SMOW}$ from 4.77 to 9.13, $^{87}Sr/^{86}Sr$ from 0.7015 to 0.70425, $^{143}Nd/^{144}Nd$ from 0.5113 to 0.5187) as well as Eu anomalies concordant with Lu/Sr ratios indicating that most of them derived from ancient, recycled, oceanic crust (e.g. Agashev et al., 2018; Jacob et al., 1994; Snyder et al., 1995, 1997). Even though no robust proof for an oceanic crustal protolith was found in some of the samples (Snyder et al., 1997), the origin of the Udachnaya eclogite suite from subducted oceanic crust is well established.

As shown in Fig. 1, bulk $\delta^{44/40}$Ca measured in two Udachnaya eclogites (0.89‰ and 0.98‰) overlap the BSE value (0.94 ± 0.05‰, Kang et al., 2017), suggesting that the recycling of subducted oceanic crust may not introduce significant Ca isotope variations to earth's mantle. The Ca isotope values in the Udachnaya eclogites are higher than in the range for normal MORB (N-MORB: 0.75–0.86‰ from Zhu et al., 2018b). These differences may be due to seawater-rock interaction, which may elevate the $\delta^{44/40}$Ca of oceanic crust (e.g., John et al., 2012), because seawater has significantly higher $\delta^{44/40}$Ca of ~1.82‰ (Fantle and Tipper, 2014). It is also possible that Ca isotope ratios in the oceanic lithosphere may evolve during subduction, e.g. via prograde metamorphism and dehydration (John et al., 2012).

5.2. Calcium isotope composition of composite Tariat xenoliths

Pyroxenites are the second most common rock type in the Earth's mantle and may play an important role in the generation of OIB type basaltic melts (e.g., Sobolev et al., 2005). The websterites and other composite xenoliths in this study were suggested to have been formed by pyroxene crystallization during the percolation of Mg-rich basaltic melts in the lithosphere (Downes, 2007; Ionov et al., 1998; Witt-Eickschen and Kramm, 1998). The $\delta^{44/40}$Ca values in the veined Tariat xenoliths are not related to modal or chemical compositions of the veins. For instance, $\delta^{44/40}$Ca in garnet orthopyroxenite 4399-24v (0.93 ± 0.10‰, n = 3, 2SD) falls in the range for spinel websterites S-12v (1.05 ± 0.16‰, n = 3, 2SD) and 4230-15v (0.88 ± 0.05‰, n = 3, 2SD). Altogether, the veins and host lherzolites, as well as hybrid lherzolite-websterite S-8, define a narrow $\delta^{44/40}$Ca range (0.88–1.05‰; Figs. 1 and 4), which overlaps the BSE estimate (0.94 ± 0.05‰) as well as the range reported for metasomatic, phlogopite-bearing Tariat lherzolites (0.88–0.89‰ in Kang et al., 2017). The narrow Ca isotope variation range in these different types of Tariat mantle rocks affected by mafic melts and metasomatic fluids suggests that these melts/fluids in the lithospheric mantle beneath Tariat had BSE-like Ca isotope compositions. Recent studies found that partial melting in the mantle causes only minor Ca isotope fractionation, with $\delta^{44/40}$Ca in the melts < 0.08‰ lighter than in the source (Kang et al., 2017; Zhang et al., 2018; Chen et al., 2019; Zhu et al., 2018b). Thus, the percolation of melts in lithospheric mantle may not significantly affect the Ca isotope of peridotites if the melts were extracted from a fertile mantle source. Moreover, the consistent $\delta^{44/40}$Ca similarities between pyroxenites and host peridotites from Tariat are in line with the conclusion of Zhang et al. (2018) and Chen et al. (2019), that the crystallization of cpx from basaltic magma causes only minor Ca isotope fractionation.

The veined Tariat xenoliths in this study were earlier analyzed for Cr isotopes (Xia et al., 2017) and yielded a very broad $\delta^{53/52}$Cr range (0.04 to −1.36‰) overlapping BSE estimates (−0.12 ± 0.10‰). Spinel websterite veins 4230-15v and S-12v have extremely low $\delta^{53/52}$Cr of −1.36 ± 0.04‰ and −0.77 ± 0.06‰, respectively, among the lowest reported for terrestrial samples and lower than in the host lherzolites (−0.09 ± 0.04‰ and −0.40 ± 0.04‰, respectively). The unusual $\delta^{53/52}$Cr values were interpreted by kinetic isotope fractionation accompanying Cr diffusion from the host to the vein during its crystallization. Mafic melts contain much less Cr than spinel peridotites, but the websterite veins formed from such melts are rich in Cr-spinel and cpx, and contain as much or more Cr than the host lherzolites. Xia et al. (2017) argued that Cr was added to the veins by diffusion from

host rocks, and that the light Cr isotope diffused faster than the heavier. By comparison, another composite Tariat xenolith, 4399-24 hosting a garnet orthopyroxenite vein, which contains no Cr-rich cpx or spinel, has a more conventional, unfractionated $\delta^{53/52}$Cr: 0.04 ± 0.04‰ in the host and −0.05 ± 0.04‰ in the vein. The stark differences between the Ca and Cr isotope compositions in the two composite Tariat xenoliths could probably be attributed to slower diffusion of 3-valent Cr^{3+} than 2-valent Ca^{2+} cations (for example, the diffusivity of Eu^{3+} is an order of magnitude slower than Eu^{2+}, Cherniak and Dimanov, 2010; Schreiber, 1977), such that any Ca isotope vein-host disequilibrium or Ca concentration gradients could be leveled during or after the vein crystallization.

5.3. Calcium isotope composition of the LH series Tok peridotites

The lithospheric mantle beneath Tok has a complex evolution history. Its fertile source experienced partial melting (possibly at ≥2 Ga; Ionov et al., 2006b), with melt extraction degrees up to 25–40%, to yield the LH series harzburgites (Ionov et al., 2005b). Shortly before the alkali basaltic eruptions in the Cenozoic, the residual mantle experienced two re-working events. First, it was percolated by mafic silica-undersaturated liquids, which converted some LH peridotites to LW series rocks recognized by high Ca/Al and FeO (Fig. 5a) and low Mg#. Then, both the remaining LH series and newly formed LW series rocks were affected by CO_2-rich media, which deposited inter-granular materials (phosphates, alkali feldspar, cpx) mainly in olivine-rich peridotites, which are most permeable for such media (Ionov et al., 2006a). To sum up, the LW series rocks are melting residues reworked by metasomatic melts; nearly all Tok peridotites also experienced late-stage metasomatism by CO_2-rich fluids.

Previous Ca isotope studies of non-metasomatized mantle xenoliths constrained the BSE $\delta^{44/40}$Ca value from data on fertile lherzolites (0.94 ± 0.05‰, 2SD) and suggested that partial melting increases the $\delta^{44/40}$Ca of residual mantle to 1.06 ± 0.04‰ (Figs. 4 and 5; Kang et al., 2017). For the two LH series rocks analyzed in this study, the $\delta^{44/40}$Ca in lherzolite 9506–1 (0.86 ± 0.07‰, n = 3, 2SD) is lower than in harzburgite 9506–0 (0.96 ± 0.10‰, n = 5, 2SD), in line with the relative magnitude of $\delta^{44/40}$Ca values in fertile and refractory mantle proposed by Kang et al. (2017). However, the $\delta^{44/40}$Ca values in these two samples are by ~0.1‰ lower than those proposed for refractory mantle by Kang et al. (2017) as seen on plots of $\delta^{44/40}$Ca vs. Mg# and CaO (Fig. 5b, c). We attribute these shifts to late-stage CO_2-rich fluid metasomatism in the Tok mantle particularly evident in harzburgite 9506–0, which contains interstitial phosphates and feldspar and is strongly LREE-enriched (e.g., $(La/Yb)_N$ ~20, Ionov et al., 2006a). The CO_2-rich fluid may be originated from recycling carbonate which have light Ca isotope compositions (e.g., Fantle and Tipper, 2014).

5.4. Light Ca isotope compositions in the Tok LW series

The $\delta^{44/40}$Ca values in the LW series rocks (0.65‰–0.87‰) overlap that for the xenolith-hosting basalt (0.70 ± 0.10‰, n = 3, 2SD), which is below the N-MORB $\delta^{44/40}$Ca range (Fig. 1). The low $\delta^{44/40}$Ca in the LW peridotites cannot be ascribed to contamination by basaltic magma because this contradicts petrographic evidence (Ionov et al., 2005a; Ionov et al., 2005b), and because some LW rocks have lower

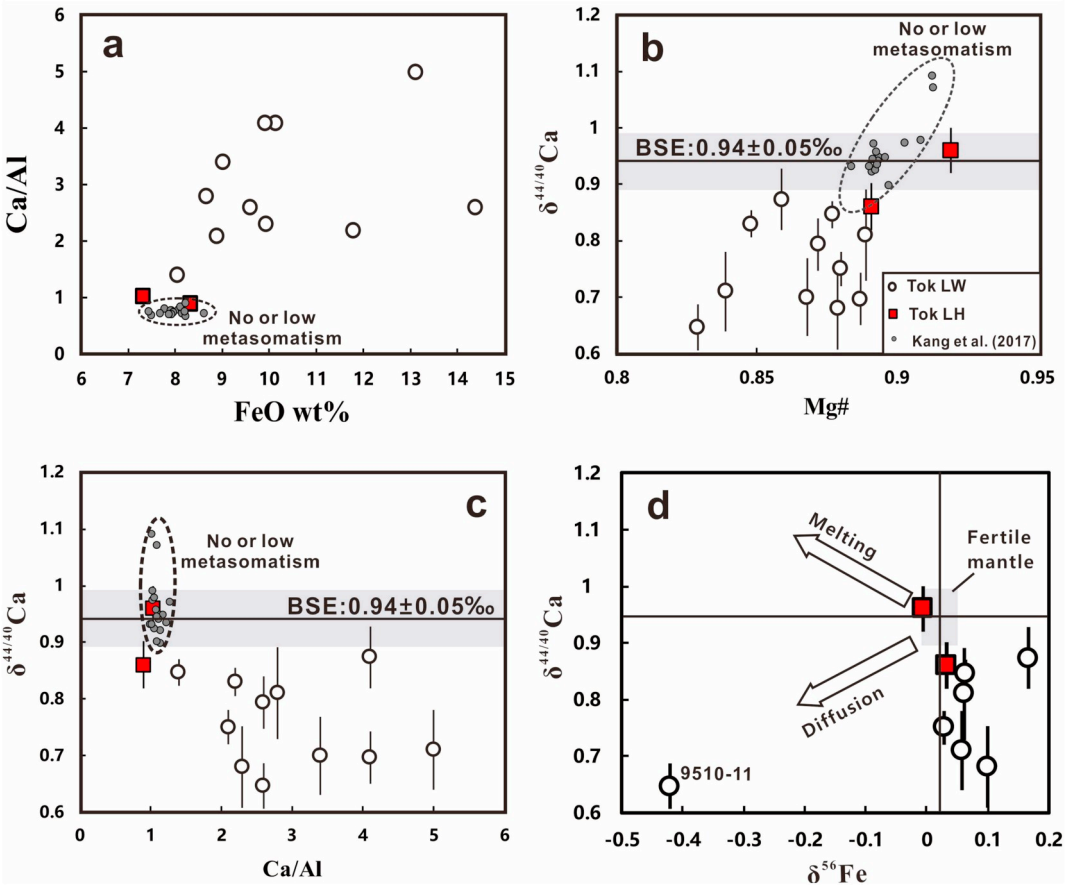

Fig. 5. Co-variation plots for major oxides and $\delta^{44/40}$Ca in the LH and LW series Tok xenoliths, and the BSE. (a) Ca/Al vs. FeO wt%; (b) $\delta^{44/40}$Ca vs. Mg#; (c) $\delta^{44/40}$Ca vs. Ca/Al. (d) $\delta^{44/40}$Ca vs. δ^{56}Fe. The Fe isotope data and fertile mantle value are from Weyer and Ionov (2007). Grey dotted line contours fertile and moderately depleted mantle peridotites (Kang et al., 2017), which experienced no or little metasomatism. Error bars are 2SE. For color codes refer to the online version of the paper.

$\delta^{44/40}$Ca than the host basalt. Moreover, the patterns and abundances of trace elements in the LW rocks are distinct from those in the basalts (Ionov et al., 2005a).

The key to explaining the Ca isotope ratios in the LW rocks is the observation that $\delta^{44/40}$Ca are negatively correlated with Ca/Al and positively correlated with Mg# (Fig. 5b, c) suggesting links between the low $\delta^{44/40}$Ca and the extent of melt metasomatism that transformed parts of residual, LH-type mantle to the Ca-Fe-rich LW series rocks. Similarities of the $\delta^{44/40}$Ca values for the host basalt, olivine-cpx cumulate (0.76 ± 0.03‰), and sample 2–1 (0.75 ± 0.03‰) which have the highest Ca/Al and FeO among the LW peridotites (products of advanced melt-rock reaction to yield olivine-cpx rocks) suggest that the evolved mafic liquids that converted the LH series to LW series rocks had $\delta^{44/40}$Ca as low as, or possibly even lower than, for the host basalt.

Another factor that could potentially contribute to the low $\delta^{44/40}$Ca in the LW series rocks is kinetic isotope fractionation. Diffusion-induced isotope overprints on metasomatized mantle peridotites have been inferred, for bulk-rocks or on a mineral scale, for several elements: Mg and Fe (Teng et al., 2011), Ca as discussed in Section 5.1 of this paper (Zhao et al., 2017), Cr (Xia et al., 2017) and Zn (Huang et al., 2018). Diffusion-related isotopic fractionation, as noted in Section 5.1, has been invoked for rocks with major element variations in minerals, which are indicative of chemical gradients during melt-rock interaction. Significant grain-to-grain FeO variations were reported for olivine in all LW series xenoliths as well as for Ca, Al, Na and Cr in pyroxenes (Ionov et al., 2005a). The most chemically heterogeneous olivine is in sample 9510-11, with FeO ranging from 12.4 to 16.6 wt% (Mg# 0.87–0.82). In addition, anomalously low δ^{56}Fe of −0.42‰ (in comparison to δ^{56}Fe of 0.02‰ inferred for fertile lherzolites, Fig. 5d) was reported for this xenolith by Weyer and Ionov (2007). This sample has the lowest $\delta^{44/40}$Ca in this study (0.65 ± 0.07‰), notably lower than in the host basalt. Overall, it is possible that kinetic isotope fractionation contributed to the low $\delta^{44/40}$Ca in this sample.

However, in this study, the hypothetical diffusion-driven Ca isotope fractionation could only be a relatively minor, supplementary or only locally important, cause for the low $\delta^{44/40}$Ca in some LW series rocks. The major factor was low $\delta^{44/40}$Ca in the metasomatic melts, which we infer from $\delta^{44/40}$Ca correlations with Fe and Ca/Al in the LW series, whereas kinetic fractionation could rather contribute to the scatter of data on these plots (Fig. 5b and c). This inference is consistent with Fe isotope data for the Tok suite (Weyer and Ionov, 2007) because, apart from sample 9510-11 with anomalously low δ^{56}Fe of −0.42‰, nine other LH and LW Tok xenoliths yield heavier δ^{56}Fe of 0.00–0.17‰ than fertile mantle of 0.02‰ ± 0.03‰ (Fig. 5d). At 1000 °C, the diffusion coefficient for Ca in silicate melt is 2.242E−12 m^2/s (Chen and Zhang, 2009), which is one order faster than Fe of 1.017E−13 m^2/s (Lowry et al., 1982). That is, the time for Ca reaching chemical equilibrium is shorter than that for Fe. If the light Ca isotope signature is caused by diffusion, Fe isotope should also be affected by diffusion and show lighter values than fertile mantle (Fig. 5d). However, such expectation is contrast with the observations on most samples (Fig. 5d). Therefore, the light Ca isotope values in the other ten LW series Tok samples (0.68 to 0.87‰), except 9510-11 were not caused by kinetic effects. Instead, we posit that the LW series rocks may have been completely or partially equilibrated with percolated melt, and that the light Ca isotope compositions mainly reflect the nature of that melt.

5.5. Light Ca isotopes in metasomatic media

Our data suggest that the low $\delta^{44/40}$Ca in the Tok peridotites, and particularly in the LW series rocks, were inherited from the Fe-Ca-rich silicate melts, with lesser contributions from related late-stage CO_2-rich fluids that metasomatized them. Such silicate melts cannot be derived from normal mantle sources because many LW series rocks have lower $\delta^{44/40}$Ca than the N-MORB (Figs. 1 and 4). The composition of the metasomatic liquid was similar, but not identical, to that of the host basalt, with significant differences in the REE and Ti (Ionov et al., 2006a). It follows that the $\delta^{44/40}$Ca in the hypothetical metasomatic melts and the host Tok basalt may not be identical either.

The LW series wehrlites have the strongest chemical imprint of the metasomatic melts. These rocks have high ratios of the middle rare earth elements (MREE) to the heavy REE (HREE), with $(Gd/Yb)_N$ from 2.2 to 4, and low Ti. Such patterns are typical of liquids generated from sources with abundant residual garnet. As discussed in Section 5.1, this study has established that garnet has higher $\delta^{44/40}$Ca than coexisting cpx, which implies that garnet-rich sources may yield partial melts enriched in light Ca isotopes if much garnet remains in the residue. Coarse garnet peridotites from the Siberian and other cratons (Doucet et al., 2013; Ionov et al., 2010) usually have low modal abundance of garnet (≤5%). Melts from such rocks may not have notably lower $\delta^{44/40}$Ca than melts from spinel peridotites. Eclogites, by contrast, contain much garnet (45–65% in Udachnaya; Agashev et al., 2018) that hosts a significant share of the whole-rock Ca (~20–40% for eclogites in this study).

An incremental fractional non-modal melting model is employed here to assess the $\delta^{44/40}$Ca of partial melts derived from eclogite sources. The results show that partial melts generated from a source with $\delta^{44/40}$Ca of 0.70 ± 0.10‰ (based on the $\delta^{44/40}$Ca of Tok host basalt) may develop $\delta^{44/40}$Ca as low as 0.53‰ (Fig. 6a). Re-working by melts derived from an eclogite source may impart both low $\delta^{44/40}$Ca and low HREE/MREE values explaining a negative correlation between $\delta^{44/40}$Ca and $(Gd/Yb)_N$ in the LW series rocks (Fig. 6b). Another argument for links of Tok metasomatic media with subducted oceanic lithosphere are chemical features of the Tok LW peridotites, like strong LREE enrichments in combination with negative Ti, Zr and Hf anomalies (Ionov et al., 2005a; Ionov et al., 2006a; Ionov et al., 2005b). It should be noticed that the modeling results are obtained based on the observations for a limited number of samples and hence more studies are required to fully understand the Ca isotope fractionation during eclogite melting.

It may not be realistic however to evoke metasomatism by pure eclogite melts because eclogite bodies may coexist with peridotites in melt sources, and because eclogite melts may react with peridotites during transport in the mantle to form mixed-source liquids. Hence, we also modeled the $\delta^{44/40}$Ca of melts generated from spinel and garnet peridotites using batch melting model at 1 GPa in Zhang et al. (2018). In both cases, the melts have $\delta^{44/40}$Ca of ~0.90‰, but garnet peridotite melts have higher $(Gd/Yb)_N$. Because eclogite melts have lower $\delta^{44/40}$Ca and higher $(Gd/Yb)_N$, their mixing with peridotite melts may explain the negative correlations between $\delta^{44/40}$Ca and $(Gd/Yb)_N$ in the LW xenoliths (Fig. 6b).

Three Tok peridotites plot above the mixing field in Fig. 6b. As discussed in Section 5.2, high $(Gd/Yb)_N$ in LH harzburgite 9506-0 are hosted by late-stage inter-granular materials deposited by metasomatic fluids, with no evidence for reworking by Ca-Fe-rich melts. The $\delta^{44/40}$Ca in this sample could be high because it is a refractory melting residue, which has higher $\delta^{44/40}$Ca than the BSE (Kang et al., 2017). A range of factors, such as a residual kinetic Ca isotope fractionation during the melt transport or metasomatic reactions could be responsible for relatively high $\delta^{44/40}$Ca in LW peridotites 3-2 and 3-22 (Fig. 6b).

5.6. Implications for Ca isotope heterogeneity of the mantle

This study shows, on the one hand, rather uniform Ca isotopic compositions in pyroxenite veins from Mongolia, and on the other hand, considerable heterogeneity for the strongly metasomatized lherzolites and wehrlites from Tok, Siberian craton. These results, together with published data on worldwide mantle rocks (Fig. 1: China, Siberian Craton, Mongolia, USA, the Alps) suggest large bulk-rock variations in the mantle, from extremely light ($\delta^{44/40}$Ca = −0.08‰) to heavy ($\delta^{44/40}$Ca = 1.85‰) (Fig. 1, Huang et al., 2010; Kang et al., 2016, 2017; Zhao et al., 2017; Chen et al., 2018, 2019). The mantle Ca isotope

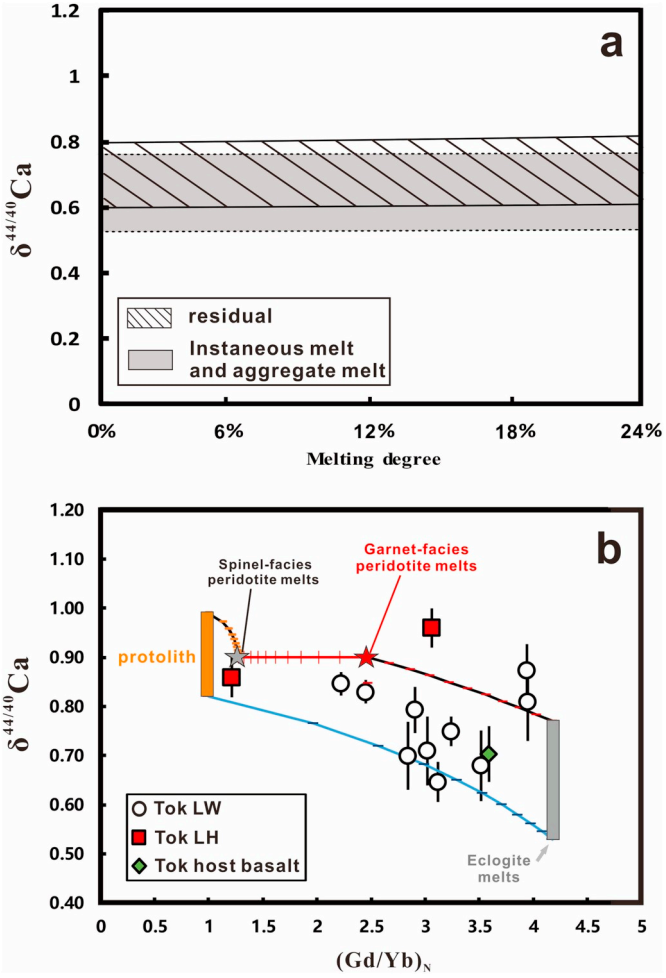

Fig.6. (a) Incremental model of $\delta^{44/40}$Ca evolution during eclogite partial melting (see Supplementary material for details). Diagonal hatching represents the range of $\delta^{44/40}$Ca in the residue; shaded area is for instantaneous and aggregate melts for initial $\delta^{44/40}$Ca of eclogite from 0.60‰ to 0.80‰, which is similar to the $\delta^{44/40}$Ca of host basalt (0.70 ± 0.10‰) and $\Delta^{44/40}Ca_{grt\text{-}cpx}$ from 0.17‰ to 0.36‰. The modeling results for instantaneous melt and aggregate melt are consistent and significantly overlap each other. (b) A plot of $\delta^{44/40}$Ca vs. $(Gd/Yb)_N$ for Tok xenoliths. The $\delta^{44/40}$Ca of presumed protoliths is set at 0.82–1.00‰ based on data for two LH rocks (lherzolite 0.86 ± 0.04‰ and harzburgite 0.96 ± 0.04‰). The melting model assumes: (i) 5% non-modal batch melting of a spinel-facies peridotite ($Ol_{0.55}$ + $Opx_{0.26}$ + $Cpx_{0.15}$ + $Spl_{0.04}$) to yield a melt mode of $Ol_{0.10}$ + $Opx_{0.27}$ + $Cpx_{0.50}$ + $Spl_{0.13}$ (McGee et al., 2013; Thirlwall et al., 1994); (ii) 5% non-modal batch melting of garnet-facies peridotite ($Ol_{0.54}$ + $Opx_{0.23}$ + $Cpx_{0.17}$ + $Grt_{0.06}$) and a melt mode of $Ol_{0.05}$ + $Opx_{0.20}$ + $Cpx_{0.30}$ + $Grt_{0.45}$ (McGee et al., 2013; Walter, 1998); 10% modal batch melting of an eclogite ($Cpx_{0.65}$ + $Grt_{0.35}$) and a melt mode of $Cpx_{0.872}$ + $Grt_{0.128}$ (Pertermann and Hirschmann, 2003). The incremental melting model yields the $\delta^{44/40}$Ca range of 0.53‰ to 0.77‰ for melts from the eclogite. The $\delta^{44/40}$Ca of melts from the garnet- and spinel-facies peridotites is set to be 0.85‰, based on N-MORB composition (Zhu et al., 2018b). The $(Gd/Yb)_N$ ratio of the BSE (Sun and McDonough, 1989) is used for the spinel- and garnet-facies peridotites, and that of the average N-MORB (Sun and McDonough, 1989) for the eclogite. Error bars are 2SE.

variations may be caused by partial melting and metasomatism (e.g., DePaolo, 2004; Huang et al., 2011; Valdes et al., 2014). The effects of partial melting are seen in non-metasomatized refractory peridotites reported by Kang et al. (2017), which have slightly heavier Ca isotope compositions than BSE estimates, as well as in our data for two LH series peridotites from Tok (0.86‰ for lherzolite 9506-1 and 0.96‰ for harzburgite 9506-0). However, melting-induced $\delta^{44/40}$Ca variations cannot exceed 0.3‰ at 30% melting according to melting models in Zhang et al. (2018) and Chen et al. (2019).

In contrast, ~1.3‰ bulk rock $\delta^{44/40}$Ca variations were observed in samples from North China and the Siberian Craton affected by mantle metasomatism, notably exceeding 0.9‰ in Fe-rich Yangyuan peridotites, North China (Zhao et al., 2017). Less spectacular, but significant are variations of 0.25‰ to 0.88‰ reported by Kang et al. (2017) for peridotites from the Siberian Craton, and ~0.3‰ variations for peridotites from North China that experienced cryptic metasomatism (Kang et al., 2016; Chen et al., 2018). More recently, ~0.3‰ Ca isotope variations were observed in carbonate-bearing metasomatized peridotites from Obnazhennaya, NE Siberian craton (Ionov et al., 2019). Overall, large Ca isotope heterogeneities in the Earth's mantle appear to be brought about mainly by mantle metasomatism.

The isotope effects of metasomatism largely depend on the nature of metasomatic agents in the lithospheric mantle. Most common of them are mafic silicate and carbonatitic melts. The latter may form by degassing of deep mantle and by recycling of subducted carbonates. Because $\delta^{44/40}$Ca of marine carbonates can be up to 2‰ lighter than for normal mantle (−1.09‰ to 1.81‰ in carbonates vs. 0.94 ± 0.05‰ of BSE, Blättler and Higgins, 2017; Fantle and Tipper, 2014), carbonatite metasomatism involving recycled carbonates was invoked to explain low $\delta^{44/40}$Ca in mantle-derived rocks such as OIBs from Hawaii (0.75‰ to 1.02‰, Huang et al., 2011), calc-alkaline basalts from the Tibetan Plateau (0.65‰ to 0.80‰, Liu et al., 2017a), refractory peridotite xenoliths from the central Siberian craton (0.25‰ to 0.96‰, Kang et al., 2017), and peridotite xenoliths from eastern China (0.76‰ to 1.04‰, Kang et al., 2016). However, many marine carbonates have heavier Ca isotopes than BSE, and the average Ca isotope composition of subducted carbonates may be similar to the BSE value (Blättler and Higgins, 2017). This is why Ionov et al. (2019) argued that recycling of marine carbonates may not alter the Ca isotope composition in global mantle, although this viewpoint needs to be tested because available data appear to suggest that carbonatite metasomatism can fractionates mantle Ca isotopes towards heavier value (Chen et al., 2018).

Pyroxenite veins in intra-plate mantle xenoliths from Mongolia in this study and in peridotite massifs exposed by plate collision in the Italian Alps (Chen et al., 2019) show Ca isotope compositions similar to BSE estimates, suggesting that intrusion of asthenosphere-derived melts does not significantly change the Ca isotope composition of mantle. In contrast, silicate melts derived from mantle sources that contain eclogites or garnet pyroxenites may have light Ca isotope composition. Such melts derived from subducted oceanic crust, or delaminated lower continental crust, may contribute light $\delta^{44/40}$Ca components both to the lithospheric mantle and basalt sources (e.g., Hauri, 1996; Huang and Frey, 2005; Sobolev et al., 2005). This mechanism may contribute to the > 0.6‰ Ca isotopic variations in OIB (see compilation in Kang et al., 2017).

6. Conclusions

We report $\delta^{44/40}$Ca data for xenoliths of mantle rocks that experienced melt intrusion (composite: peridotites cut by pyroxenite veins) or infiltration (reactive wehrlites) as well as for eclogites and their minerals. Garnet in eclogites from Udachnaya has higher $\delta^{44/40}$Ca than coexisting cpx, with $\Delta^{44/40}Ca_{grt\text{-}cpx}$ from 0.22 ± 0.11‰ to 0.34 ± 0.04‰. We ascribe this difference to equilibrium isotope fractionation controlled by mineral structures.

The composite peridotite xenoliths from Mongolia show a narrow $\delta^{44/40}$Ca range both in the host lherzolites and in crosscutting pyroxenite veins (0.88–1.05‰) that overlaps the BSE value (0.94 ± 0.05‰). This suggests that the parental liquids of the pyroxenites had BSE-like $\delta^{44/40}$Ca values, and that Ca isotope compositions are little affected by diffusion-related kinetic isotope fractionation during vein formation, by contrast to isotopes of 3-valent Cr, which may reflect the faster diffusion rate of Ca than that of 3-valent Cr.

The $\delta^{44/40}$Ca range in the LH series Tok peridotites (0.86–0.96‰) may reflect combined effects of partial melting and limited fluid-related metasomatism. The LW series Tok peridotites that formed by re-working of refractory peridotites by Ca-Fe-enriched silicate melts show a generally lighter $\delta^{44/40}$Ca range (0.65–0.87‰), with $\delta^{44/40}$Ca correlated with Ca/Al, FeO and $(Gd/Yb)_N$. We can explain these observations by reaction of their refractory protoliths with low-$\delta^{44/40}$Ca melts generated from mixed eclogite and peridotite sources, with no, or very limited, kinetic isotope fractionation.

Acknowledgements

We thank Shuijiong Wang for discussions and Gui-Qin Wang and Xin Li for analytical assistance. Tariat xenoliths S8 and S12 were collected by R. W. Carlson and D. A. Ionov supported by NSF Grant EAR-1009494 to RWC. This work was supported by the Strategic Priority Research Program (B) of the Chinese Academy of Sciences (XDB18000000), the National Science Foundation of China (41873002, 41373007, 41325011, 41573017, 41773009) and the N°111 Plan. DAI acknowledges the Visiting Scientist fellowships within the CAS (Chinese Academy of Sciences) President's International Fellowship Initiative (PIFI) in 2017–19 (Grant No. 2017VCA0009).

Appendix A. Supplementary data

Supplementary data to this article can be found online at https://doi.org/10.1016/j.chemgeo.2019.06.010.

References

Agashev, A., Pokhilenko, L., Pokhilenko, N., Shchukina, E., 2018. Geochemistry of eclogite xenoliths from the Udachnaya Kimberlite Pipe: section of ancient oceanic crust sampled. Lithos 314, 187–200.
Amini, M., Eisenhauer, A., Böhm, F., Holmden, C., Kreissig, K., Hauff, F., Jochum, K.P., 2009. Calcium isotopes ($\delta^{44}/^{40}$Ca) in MPI-DING reference glasses, USGS rock powders and various rocks: evidence for Ca isotope fractionation in terrestrial silicates. Geostand. Geoanal. Res. 33, 231–247.
Antonelli, M.A., Schiller, M., Schauble, E.A., Mittal, T., DePaolo, D.J., Chacko, T., Grew, E.S., Tripoli, B., 2019. Kinetic and equilibrium Ca isotope effects in high-T rocks and minerals. Earth Planet. Sci. Lett. 517, 71–82.
Bailey, D., 1982. Mantle metasomatism—continuing chemical change within the Earth. Nature 296, 525–530.
Beran, A., Libowitzky, E., Armbruster, T., 1996. A single-crystal infrared spectroscopic and X-ray-diffraction study of untwinned San Benito perovskite containing OH groups. Can. Mineral. 34, 803–809.
Blättler, C.L., Higgins, J.A., 2017. Testing Urey's carbonate–silicate cycle using the calcium isotopic composition of sedimentary carbonates. Earth Planet. Sci. Lett. 479, 241–251.
Bodinier, J.-L., Godard, M., 2003. Orogenic, ophiolitic, and abyssal peridotites. In: Treatise on Geochemistry. vol. 2. pp. 568.
Bodinier, J., Vasseur, G., Vernieres, J., Dupuy, C., Fabries, J., 1990. Mechanisms of mantle metasomatism: geochemical evidence from the Lherz orogenic peridotite. J. Petrol. 31, 597–628.
Cameron, M., Sueno, S., Prewitt, C.T., Papike, J.J., 1973. High-temperature crystal chemistry of acmite, diopside, hedenbergite, jadeite, spodumene, and ureyite. Am. Mineral. 58, 594–618.
Chen, Y., Zhang, Y., 2009. Clinopyroxene dissolution in basaltic melt. Geochimica et Cosmochimica Acta 73, 5730–5747.
Chen, C., Liu, Y., Feng, L., Foley, S.F., Zhou, L., Ducea, M.N., Hu, Z., 2018. Calcium isotope evidence for subduction-enriched lithospheric mantle under the northern North China Craton. Geochim. Cosmochim. Acta 238, 55–67.
Chen, C., Dai, W., Wang, Z., Liu, Y., Li, M., Becker, H., Foley, S.F., 2019. Calcium isotope fractionation during magmatic processes in the upper mantle. Geochim. Cosmochim. Acta 249, 121–137.
Cherniak, D., Dimanov, A., 2010. Diffusion in pyroxene, mica and amphibole. Rev. Mineral. Geochem. 72, 641–690.
DePaolo, D.J., 2004. Calcium isotopic variations produced by biological, kinetic, radiogenic and nucleosynthetic processes. Rev. Mineral. Geochem. 55, 255–288.
Doucet, L.S., Ionov, D.A., Golovin, A.V., 2013. The origin of coarse garnet peridotites in cratonic lithosphere: new data on xenoliths from the Udachnaya kimberlite, central Siberia. Contrib. Mineral. Petrol. 165, 1225–1242.
Downes, H., 2007. Origin and significance of spinel and garnet pyroxenites in the shallow lithospheric mantle: ultramafic massifs in orogenic belts in Western Europe and NW Africa. 99, 1–24.
Fantle, M.S., Tipper, E.T., 2014. Calcium isotopes in the global biogeochemical Ca cycle: implications for development of a Ca isotope proxy. Earth Sci. Rev. 129, 148–177.
Feng, C., Qin, T., Huang, S., Wu, Z., Huang, F., 2014. First-principles investigations of equilibrium calcium isotope fractionation between clinopyroxene and Ca-doped orthopyroxene. Geochim. Cosmochim. Acta 143, 132–142.
Hauri, E.H., 1996. Major-element variability in the Hawaiian mantle plume. Nature 382, 415.
He, Y., Wang, Y., Zhu, C., Huang, S., Li, S., 2017. Mass-independent and mass-dependent Ca isotopic compositions of thirteen geological reference materials measured by thermal ionisation mass spectrometry. Geostand. Geoanal. Res. 41, 283–302.
Heuser, A., Eisenhauer, A., Gussone, N., Bock, B., Hansen, B., Nägler, T.F., 2002. Measurement of calcium isotopes (δ^{44}Ca) using a multicollector TIMS technique. Int. J. Mass Spectrom. 220, 385–397.
Huang, S., Frey, F.A., 2005. Recycled oceanic crust in the Hawaiian Plume: evidence from temporal geochemical variations within the Koolau Shield. Contrib. Mineral. Petrol. 149, 556–575.
Huang, X.-L., Xu, Y.-G., Lo, C.-H., Wang, R.-C., Lin, C.-Y., 2007. Exsolution lamellae in a clinopyroxene megacryst aggregate from Cenozoic basalt, Leizhou Peninsula, South China: petrography and chemical evolution. Contrib. Mineral. Petrol. 154, 691–705.
Huang, S., Farkaš, J., Jacobsen, S.B., 2010. Calcium isotopic fractionation between clinopyroxene and orthopyroxene from mantle peridotites. Earth Planet. Sci. Lett. 292, 337–344.
Huang, S., Farkaš, J., Jacobsen, S.B., 2011. Stable calcium isotopic compositions of Hawaiian shield lavas: evidence for recycling of ancient marine carbonates into the mantle. Geochim. Cosmochim. Acta 75, 4987–4997.
Huang, J., Chen, S., Zhang, X.C., Huang, F., 2018. Effects of melt percolation on Zn isotope heterogeneity in the mantle: constraints from peridotite massifs in Ivrea-Verbano Zone, Italian Alps. J. Geophys. Res. Solid Earth 123, 2706–2722.
Huang, F., Zhou, C., Wang, W., Kang, J., Wu, Z., 2019. First-principles calculations of equilibrium Ca isotope fractionation: implications for oldhamite formation and evolution of lunar magma ocean. Earth Planet. Sci. Lett. 510, 153–160.
Ionov, D.A., Dupuy, C., O'Reilly, S.Y., Kopylova, M.G., Genshaft, Y.S., 1993. Carbonated peridotite xenoliths from Spitsbergen: implications for trace element signature of mantle carbonate metasomatism. Earth Planet. Sci. Lett. 119, 283–297.
Ionov, D.A., O'Reilly, S.Y., Genshaft, Y.S., Kopylova, M.G., 1996. Carbonate-bearing mantle peridotite xenoliths from Spitsbergen: phase relationships, mineral compositions and trace-element residence. Contrib. Mineral. Petrol. 125, 375–392.
Ionov, D.A., O'Reilly, S.Y., Griffin, W.L., 1998. A geotherm and lithospheric section for central Mongolia (Tariat region). Mantle dynamics and plate interactions in East Asia. Geodyn. Ser 27, 127–153.
Ionov, D.A., Chanefo, I., Bodinier, J.-L., 2005a. Origin of Fe-rich lherzolites and wehrlites from Tok, SE Siberia by reactive melt percolation in refractory mantle peridotites. Contrib. Mineral. Petrol. 150, 335–353.
Ionov, D.A., Prikhodko, V.S., Bodinier, J.-L., Sobolev, A.V., Weis, D., 2005b. Lithospheric mantle beneath the south-eastern Siberian craton: petrology of peridotite xenoliths in basalts from the Tokinsky Stanovik. Contrib. Mineral. Petrol. 149, 647–665.
Ionov, D.A., Chazot, G., Chauvel, C., Merlet, C., Bodinier, J.-L., 2006a. Trace element distribution in peridotite xenoliths from Tok, SE Siberian craton: a record of pervasive, multi-stage metasomatism in shallow refractory mantle. Geochim. Cosmochim. Acta 70, 1231–1260.
Ionov, D.A., Shirey, S.B., Weis, D., Brügmann, G., 2006b. Os–Hf–Sr–Nd isotope and PGE systematics of spinel peridotite xenoliths from Tok, SE Siberian craton: effects of pervasive metasomatism in shallow refractory mantle. Earth Planet. Sci. Lett. 241, 47–64.
Ionov, D.A., Doucet, L.S., Ashchepkov, I.V., 2010. Composition of the lithospheric mantle in the Siberian craton: new constraints from fresh peridotites in the Udachnaya-East Kimberlite. J. Petrol. 51, 2177–2210.
Ionov, D.A., Carlson, R.W., Doucet, L.S., Golovin, A.V., Oleinikov, O.B., 2015. The age and history of the lithospheric mantle of the Siberian craton: Re–Os and PGE study of peridotite xenoliths from the Obnazhennaya kimberlite. Earth Planet. Sci. Lett. 428, 108–119.
Ionov, D.A., Qi, Y.-H., Kang, J.-T., Golovin, A.V., Oleinikov, O.B., Zheng, W., Anbar, A.D., Zhang, Z.-F., Huang, F., 2019. Calcium isotopic signatures of carbonatite and silicate metasomatism, melt percolation and crustal recycling in the lithospheric mantle. Geochim. Cosmochim. Acta 248, 1–13.
Jacob, D., Jagoutz, E., Lowry, D., Mattey, D., Kudrjavtseva, G., 1994. Diamondiferous eclogites from Siberia: remnants of Archean oceanic crust. Geochim. Cosmochim. Acta 58, 5191–5207.
John, T., Gussone, N., Podladchikov, Y.Y., Bebout, G.E., Dohmen, R., Halama, R., Klemd, R., Magna, T., Seitz, H.-M., 2012. Volcanic arcs fed by rapid pulsed fluid flow through subducting slabs. Nat. Geosci. 5, 489.
Kang, J.-T., Zhu, H.-L., Liu, Y.-F., Liu, F., Wu, F., Hao, Y.-T., Zhi, X.-C., Zhang, Z.-F., Huang, F., 2016. Calcium isotopic composition of mantle xenoliths and minerals from Eastern China. Geochim. Cosmochim. Acta 174, 335–344.
Kang, J.-T., Ionov, D.A., Liu, F., Zhang, C.-L., Golovin, A.V., Qin, L.-P., Zhang, Z.-F., Huang, F., 2017. Calcium isotopic fractionation in mantle peridotites by melting and metasomatism and ca isotope composition of the Bulk Silicate Earth. Earth Planet. Sci. Lett. 474, 128–137.
Liu, F., Li, X., Wang, G., Liu, Y., Zhu, H., Kang, J., Huang, F., Sun, W., Xia, X., Zhang, Z., 2017a. Marine carbonate component in the mantle beneath the southeastern Tibetan Plateau: evidence from magnesium and calcium isotopes. J. Geophys. Res. Solid Earth 9729–9744.
Liu, F., Zhu, H.L., Li, X., Wang, G.Q., Zhang, Z.F., 2017b. Calcium isotopic fractionation and compositions of geochemical reference materials. Geostand. Geoanal. Res. 41, 675–688.
Lowry, R.K., Henderson, P., Nolan, J., 1982. Tracer diffusion of some alkali, alkaline-earth and transition element ions in a basaltic and an andesitic melt, and the implications concerning melt structure. Contrib. Mineral. Petrol. 80, 254–261.

Macris, C.A., Manning, C.E., Young, E.D., 2015. Crystal chemical constraints on inter-mineral Fe isotope fractionation and implications for Fe isotope disequilibrium in San Carlos mantle xenoliths. Geochim. Cosmochim. Acta 154, 168–185.
Magna, T., Gussone, N., Mezger, K., 2015. The calcium isotope systematics of Mars. Earth Planet. Sci. Lett. 430, 86–94.
McGee, L.E., Smith, I.E., Millet, M.-A., Handley, H.K., Lindsay, J.M., 2013. Asthenospheric control of melting processes in a monogenetic basaltic system: a case study of the Auckland Volcanic Field, New Zealand. J. Petrol. 54, 2125–2153.
Moyen, J.-F., Paquette, J.-L., Ionov, D., Gannoun, A., Korsakov, A., Golovin, A., Moine, B., 2017. Paleoproterozoic rejuvenation and replacement of Archaean lithosphere: evidence from zircon U–Pb dating and Hf isotopes in crustal xenoliths at Udachnaya, Siberian craton. Earth Planet. Sci. Lett. 457, 149–159.
Pertermann, M., Hirschmann, M.M., 2003. Anhydrous partial melting experiments on MORB-like eclogite: phase relations, phase compositions and mineral–melt partitioning of major elements at 2–3 GPa. J. Petrol. 44, 2173–2201.
Ravna, K., 2000. The garnet–clinopyroxene Fe^{2+}–Mg geothermometer: an updated calibration. J. Metamorph. Geol. 18, 211–219.
Richter, F.M., Watson, E.B., Mendybaev, R., Dauphas, N., Georg, B., Watkins, J., Valley, J., 2009. Isotopic fractionation of the major elements of molten basalt by chemical and thermal diffusion. Geochim. Cosmochim. Acta 73, 4250–4263.
Rudnick, R.L., McDonough, W.F., Chappell, B.W., 1993. Carbonatite metasomatism in the northern Tanzanian mantle: petrographic and geochemical characteristics. Earth Planet. Sci. Lett. 114, 463–475.
Schauble, E.A., 2011. First-principles estimates of equilibrium magnesium isotope fractionation in silicate, oxide, carbonate and hexaaquamagnesium (2+) crystals. Geochim. Cosmochim. Acta 75, 844–869.
Schreiber, H.D., 1977. Redox states of Ti, Zr, Hf, Cr, and EU in basaltic magmas-an experimental study. In: Lunar and Planetary Science Conference Proceedings, pp. 1785–1807.
Sharp, Z., Hazen, R., Finger, L., 1987. High-pressure crystal chemistry of monticellite, $CaMgSiO_4$. Am. Mineral. 72, 748–755.
Snyder, G.A., Taylor, L.A., Jerde, E.A., Clayton, R.N., Mayeda, T.K., Deines, P., Rossman, G.R., Sobolev, N.V., 1995. Archean mantle heterogeneity and the origin of diamondiferous eclogites, Siberia: evidence from stable isotopes and hydroxyl in garnet. Am. Mineral. 80, 799–809.
Snyder, G.A., Taylor, L.A., Crozaz, G., Halliday, A.N., Beard, B.L., Sobolev, V.N., Sobolev, N.V., 1997. The origins of Yakutian eclogite xenoliths. J. Petrol. 38, 85–113.
Sobolev, A.V., Hofmann, A.W., Sobolev, S.V., Nikogosian, I.K., 2005. An olivine-free mantle source of Hawaiian shield basalts. Nature 434, 590.
Sun, S.-S., McDonough, W.F., 1989. Chemical and isotopic systematics of oceanic basalts: implications for mantle composition and processes. Geol. Soc. Lond., Spec. Publ. 42, 313–345.
Teng, F.-Z., Dauphas, N., Helz, R.T., Gao, S., Huang, S., 2011. Diffusion-driven magnesium and iron isotope fractionation in Hawaiian olivine. Earth Planet. Sci. Lett. 308, 317–324.
Thirlwall, M., Upton, B., Jenkins, C., 1994. Interaction between continental lithosphere and the Iceland plume—Sr-Nd-Pb isotope geochemistry of Tertiary basalts, NE Greenland. J. Petrol. 35, 839–879.
Urey, H.C., 1947. The thermodynamic properties of isotopic substances. J. Chem. Soc. 562–581.
Valdes, M.C., Moreira, M., Foriel, J., Moynier, F., 2014. The nature of Earth's building blocks as revealed by calcium isotopes. Earth Planet. Sci. Lett. 394, 135–145.
Walter, M.J., 1998. Melting of garnet peridotite and the origin of komatiite and depleted lithosphere. J. Petrol. 39, 29–60.
Wang, W., Qin, T., Zhou, C., Huang, S., Wu, Z., Huang, F., 2017a. Concentration effect on equilibrium fractionation of Mg-Ca isotopes in carbonate minerals: insights from first-principles calculations. Geochim. Cosmochim. Acta 208, 185–197.
Wang, W., Zhou, C., Qin, T., Kang, J.-T., Huang, S., Wu, Z., Huang, F., 2017b. Effect of Ca content on equilibrium Ca isotope fractionation between orthopyroxene and clinopyroxene. Geochim. Cosmochim. Acta 219, 44–56.
Weyer, S., Ionov, D.A., 2007. Partial melting and melt percolation in the mantle: the message from Fe isotopes. Earth Planet. Sci. Lett. 259, 119–133.
Witt-Eickschen, G., Kramm, U., 1998. Evidence for the multiple stage evolution of the subcontinental lithospheric mantle beneath the Eifel (Germany) from pyroxenite and composite pyroxenite/peridotite xenoliths. Contrib. Mineral. Petrol. 131, 258–272.
Xia, J., Qin, L., Shen, J., Carlson, R.W., Ionov, D.A., Mock, T.D., 2017. Chromium isotope heterogeneity in the mantle. Earth Planet. Sci. Lett. 464, 103–115.
Yaxley, G.M., Crawford, A.J., Green, D.H., 1991. Evidence for carbonatite metasomatism in spinel peridotite xenoliths from western Victoria, Australia. Earth Planet. Sci. Lett. 107, 305–317.
Young, E.D., Tonui, E., Manning, C.E., Schauble, E., Macris, C.A., 2009. Spinel–olivine magnesium isotope thermometry in the mantle and implications for the Mg isotopic composition of Earth. Earth Planet. Sci. Lett. 288, 524–533.
Zhang, H., Wang, Y., He, Y., et al., 2018. No measurable calcium isotopic fractionation during crystallization of Kilauea Iki lava lake. Geochem. Geophys. Geosyst. 19 (9), 3128–3139.
Zhao, X., Zhang, Z., Huang, S., Liu, Y., Li, X., Zhang, H., 2017. Coupled extremely light Ca and Fe isotopes in peridotites. Geochim. Cosmochim. Acta 208, 368–380.
Zhou, C., Wang, W., Kang, J., Wu, Z., Huang, F., 2016. First-principles calculations of equilibrium calcium isotope fractionation among Ca-bearing minerals. In: AGU Fall Meeting Abstracts.
Zhu, H., Zhang, Z.F., Wang, G.Q., Liu, Y.F., Liu, F., Li, X., Sun, W.D., 2016. Calcium isotopic fractionation during ion-exchange column chemistry and thermal ionisation mass spectrometry (TIMS) determination. Geostand. Geoanal. Res. 40, 185–194.
Zhu, H., Liu, F., Li, X., An, Y., Wang, G., Zhang, Z., 2018a. A “peak cut” procedure of column separation for calcium isotope measurement using the double spike technique and thermal ionization mass spectrometry (TIMS). J. Anal. At. Spectrom. 33 (4), 547–554.
Zhu, H., Liu, F., Li, X., Wang, G., Zhang, Z., Sun, W., 2018b. Calcium isotopic compositions of normal mid-ocean ridge basalts from the Southern Juan de Fuca Ridge. J. Geophys. Res. Solid Earth 123 (2), 1303–1313.
Ziberna, L., Nimis, P., Kuzmin, D., Malkovets, V.G., 2016. Error sources in single-clinopyroxene thermobarometry and a mantle geotherm for the Novinka kimberlite, Yakutia. Am. Mineral. 101, 2222–2232.